X-ray-photon scattering by an excited and ionized atom

Alexey N. Hopersky, Alexey M. Nadolinsky,* Sergey A. Novikov, and Victor A. Yavna
Chair of Mathematics, Rostov State University of TC, Rostov-on-Don 344038, Russia
(Received 31 August 2014; published 17 February 2015)

The scattering process of an x-ray photon by an excited and ionized many-electron atom with attosecond photon-electron contact interaction is theoretically investigated. The results of the authors' recent work [Hopersky *et al.*, Phys. Rev. A **88**, 032704 (2013)] are generalized for the cases of (a) arbitrary energy of the photon that prepares the scattering state and (b) the scattering of the photon by the continuous spectrum electron of the ionization state of the atom. The atom of Ne is considered as the object of the study. Along with the effects of normal Compton and elastic scattering, the existence of anomalous inelastic scattering is predicted. It may be assumed that this effect will become a basis for an experimental method of increasing the energy of the photons generated, for example, by a free-electron x-ray laser. It is determined that during the elastic scattering of a photon by an electron of the continuous spectrum, along with the known contribution from the j_l Bessel function over the $l = 0$ harmonic (Thomson scattering), there is also a contribution from Bessel functions with harmonics $l \in [1;\infty)$. The experimental discovery and application of the anomalous Compton photon scattering effect directly by the atomic electron of the continuous spectrum have their own practical interest.

DOI: 10.1103/PhysRevA.91.022708 PACS number(s): 34.50.−s, 31.30.J−, 32.30.Rj, 32.80.−t

I. INTRODUCTION

Current experimental capabilities of the x-ray free-electron laser ([1], and references therein) and of the inverse Compton scattering of a photon by a high-energy beam of free electrons ([2], and references therein) open up the possibility of investigating fundamental nonlinear processes of the interaction between a photon and a many-electron system with a high degree of spectral resolution. One of these processes, in particular, is the scattering of an x-ray photon $\hbar\omega_1$ ($\hbar$ is Planck's constant, ω_1 is the angular frequency of the photon) by an excited and ionized atom with attosecond (1 as $= 10^{-3}$ fs $= 10^{-18}$ s) duration of the photon-electron interaction.

We recently performed a theoretical investigation of the double-differential cross section $[d^2\sigma/d(\hbar\omega_2)d\Omega_2$; $\hbar\omega_2$ is energy and Ω_2 is the solid angle of flight of the scattered photon] of this process [3] for the beryllium atom (Be: nuclear charge is $Z = 4$, configuration and ground-state term are $[0] = 1s^22s^2[^1S_0]$). We determined that with the duration of interaction between the photons and the excited atom much smaller than the lifetime of the $1s$ vacancy, the quantum effect of anomalous ($\omega_2 > \omega_1$) inelastic scattering of the photon by the previously excited many-electron system is realized. The consideration was limited only to the $1s2s^2np[^1P_1]$, $n \geqslant 2$ states of the discrete spectrum with energies fixed as the energies of photoexcitation thresholds: $\hbar\omega_0 = I_{1snp}$. Here, $\hbar\omega_0$ is the energy of the photon preparing the excited states as the initial scattering states and I_{1snp} is the energy of the threshold of $1s \to np$ photoexcitation. We also did not consider the scattering processes of the $\hbar\omega_1$ photon by the $1s2s^2\varepsilon p[^1P_1]$ states of the continuous spectrum. The inclusion of the latter, as will be shown, leads to the discovery of new quantum effects in the processes of scattering of a photon by an excited and ionized atom, which was not studied in [3].

In this work we relax the mentioned constraints of [3] and construct a general nonrelativistic quantum theory of triple-differential scattering cross section $[d^3\sigma/d(\hbar\omega_0)\,d(\hbar\omega_2)\,d\Omega_2]$ of a photon by an excited and ionized atom with attosecond duration of the contact interaction between the photons and the atom for arbitrary energy of the $\hbar\omega_0$ photon. As an example, we consider the atom of neon (Ne: $Z = 10$, $[0] = 1s^22s^22p^6[^1S_0]$). In this case, the condition of applicability of the type of quantum perturbation theory developed by us, $\hbar|E_0 + I_{1s}|^{-1} \ll \tau \ll \tau_{1s}$ [4], takes the form of 0.25 as $\ll \tau \ll 2.44$ fs. Here, E_0 is the energy of the atomic ground state, I_{1s} is the energy of the ionization threshold of the $1s^2$ atomic shell, τ is the duration of the contact interaction between the photons and the atom, and $\tau_{1s} = \hbar\Gamma_{1s}^{-1}$ is the lifetime of the $1s$ vacancy. Quantities $E_0 = -3497.86$ eV and $I_{1s} = 868.39$ eV are obtained in this work. For the natural decay linewidth of the $1s$ vacancy, $\Gamma_{1s}(1s \to np) = 0.24$ eV [5] and $\Gamma_{1s}(1s \to \varepsilon p) = 0.27$ eV [6] are taken. According to, e.g., [7] ($\hbar\omega_1 = 10$ keV, $\tau = 50$ as) and [8] ($\hbar\omega_1 = 1.6$ keV, $\tau = 2.5$ as) the above double inequality may be realized experimentally. As a result, one can expect the experimental discovery of the quantum effects predicted in [3] and in this work when a photon is scattered by a previously excited and ionized many-electron system.

II. THEORY

The attempt to represent the process of "merging" of $\hbar\omega_0$ and $\hbar\omega_1$ photons via the $\hbar\omega_0 + \hbar\omega_1 + [0] \to [0] + \hbar\omega_2$ channel is forbidden by the Landau-Yang theorem [9] of quantum electrodynamics about the conservation of the total spin of a two-photon system. In this case with the $^1S_0$ term of the atomic ground state $s(\omega_0) \oplus s(\omega_1) = 0$ (or 2) $\neq s(\omega_2) = 1$. Therefore let us consider the investigated here scattering of the $\hbar\omega_1$ photon by a previously excited and ionized atom as a two-step process.

First step. The $\hbar\omega_0$ photon excites and ionizes the atom into states $1s2s^22p^6(n,\varepsilon)p$,

$$\hbar\omega_0 + [0] \to 1s2s^22p^6(n,\varepsilon)p[^1P_1], \qquad (1)$$

*amnrnd@mail.ru

and thus prepares (creates) the initial scattering states. The probability amplitude for the excitation and ionization of the atom is determined by the matrix element of the radiative transition operator:

$$\widehat{R} = -\frac{e}{m_e c}\sum_{i=1}^{N}(\widehat{p}_i \cdot \widehat{A}_i). \tag{2}$$

In Eq. (2) e is the electron charge, m_e is the electron mass, c is the speed of light in vacuum, $\widehat{A}_i \equiv \widehat{A}(t;\vec{r}_i)$ is the electromagnetic field operator in the second-quantization representation, t is the field propagation time, $\vec{r}_i$ is the radius vector, $\widehat{p}_i$ is the momentum operator of the ith atomic electron, and N is the number of electrons in the atom.

Second step. The $\hbar\omega_1$ photon is scattered by $1s2s^22p^6(n,\varepsilon)p$ states over the channels:

$$\hbar\omega_1 + 1s2s^22p^6(n,\varepsilon)p \to C + \hbar\omega_2, \tag{3}$$

where the structures of C configurations of the final scattering states will be specified in Sec. III. The probability amplitude of scattering is determined by the matrix element of the contact interaction operator nonlinear with respect to the electromagnetic field:

$$\widehat{Q} = \frac{1}{2m_e}\left(\frac{e}{c}\right)^2\sum_{i=1}^{N}(\widehat{A}_i \cdot \widehat{A}_i). \tag{4}$$

The notion of "contactness" of the $\widehat{Q}$ operator means that operators of the electromagnetic field in Eq. (4) and the single-electron transition wave functions are taken in the same space-time point (see Fig. 2). The nonlinearity in the $\widehat{Q}$ operator over the field, even in the first order of the nonrelativistic perturbation theory, determines the existence of quantum effects of both normal ($\omega_2 \leqslant \omega_1$), and anomalous ($\omega_2 > \omega_1$) scattering. Of course, the $\widehat{R}$ operator also determines two-photon processes, but already in the second order of the perturbation theory. Consideration of such processes with the participation of the $\widehat{R}$ operator is the subject of future research.

Then, the analytical structure of the total triple-differential scattering cross section ($d^3\sigma/d\omega_0\ d\omega_2\ d\Omega_2 \equiv \sigma^{(3)}$) of the ω_1 photon by the excited and ionized atom reproduces the statement of the well-known [10] theorem of total probability, but in a generalized [integral, see Eq. (11)] form:

$$\sigma^{(3)} = \sum_{n>f}^{\infty}\rho_n\sigma_n^{(3)} + \rho_c\sigma_c^{(3)}. \tag{5}$$

In Eq. (5) and below, the atomic system of units is used ($e = m_e = \hbar = 1$), and $\sigma_n^{(3)}$ ($\sigma_c^{(3)}$) are defined as the partial triple-differential cross sections over the $1s2s^22p^6np$ ($1s2s^22p^6\varepsilon p$) states of the discrete (continuous) spectrum, f is the Fermi level (set of quantum numbers of the atomic valence shell in the ground state [0]). Indeed, from the point of view of interpreting the total probability theorem in Eq. (5), a correspondence is defined: $\sigma^{(3)} \sim P(A)$ is the probability of event A (scattering of the photon ω_1); the probability of the first step as $\rho_{n,c} \sim P(H_{n,c})$, the probability of hypothesis $H_{n,c}$ [creation of the $1s2s^22p^6np$ ($1s2s^22p^6\varepsilon p$) state]; and the probability of the second step as $\sigma_{n,c}^{(3)} \sim P(A/H_{n,c})$, the conditional probability of event A after the realization of hypothesis $H_{n,c}$.

According to this correspondence, probabilities $\rho_n < 1$ and $\rho_c < 1$ ($\rho_n \to 0$ and $\rho_c \to 1$ as $\omega_0 \to \infty$) are expressed via the squares of the matrix elements of the $\widehat{R}$ operator:

$$\rho_n = \sigma_n/\sigma = P_n/D, \tag{6}$$

$$\rho_c = \sigma_c/\sigma = \eta/D, \tag{7}$$

$$\sigma = \sum_{n>f}^{\infty}\sigma_n + \sigma_c\,, \tag{8}$$

$$D = \sum_{m>f}^{\infty}P_m + \eta. \tag{9}$$

In Eqs. (6)–(9) the following quantities are defined:

$$P_n = M_n^2 L_n, \tag{10}$$

$$\eta = (1/\omega_0)\int_0^{\infty}(x + I_{1s})M^2(x)L(x)\,dx, \tag{11}$$

$$M_n = \langle 1s|\hat{r}|np\rangle, \tag{12}$$

$$M(x) = \langle 1s|\hat{r}|xp\rangle, \tag{13}$$

$$L_n = (\gamma_{1s}/\pi)\left[(\omega_0 - I_{1snp})^2 + \gamma_{1s}^2\right]^{-1}, \tag{14}$$

$$L(x) = (\gamma_{1s}/\pi)\left[(\omega_0 - I_{1s} - x)^2 + \gamma_{1s}^2\right]^{-1}. \tag{15}$$

In Eqs. (6)–(15) σ_n (σ_c) is the cross section of the single $1s \to np$ ($1s \to \varepsilon p$) excitation (ionization) of the $1s^2$ atomic shell [11], M_n [$M(x)$] is radial part of the probability amplitude (in Dirac's notation [4]) of the $1s \to np$ ($1s \to \varepsilon p$) transition in the dipole approximation for the $\widehat{R}$ operator, L_n and $L(x)$ are Cauchy-Lorentz spectral functions (spectral densities of states), and $\gamma_{1s} = \Gamma_{1s}/2$. Let us note that the use of the dipole approximation for the $\widehat{R}$ operator is justified by the satisfaction of the inequality $\lambda \gg r_{nl}$. Here, λ is the wavelength of the absorbed ω_0 photon, and r_{nl} is the average radius of the nl atomic shell that determines the radiative transition integral. In our case for ω_0 from 850 to 900 eV (λ from 14.6 to 13.8 Å) we have $\lambda \gg r_{1s}(\mathrm{Ne}) = 0.08$ Å. As expected, for arbitrary energy of the ω_0 photon, the condition of completeness of the hypothesis set [10] is satisfied:

$$\sum_{n>f}^{\infty}\rho_n + \rho_c = 1. \tag{16}$$

Functions ρ_n and ρ_c for the Ne atom are shown in Fig. 1. Violation of equality (16) in the region of energies $\omega_0 \leqslant I_{1s}$ is due to the fact that we limited the number of photoexcitation states to those with $n \leqslant 10$ out of the full set of $n \in [3;\infty)$. In Figs. 3–5 the violation of equality (16) leads to the loss of scattering intensity in the region of energies $\omega_0 \leqslant I_{1s}$. In our other work [12] it is shown that for the Ne atom, a similar

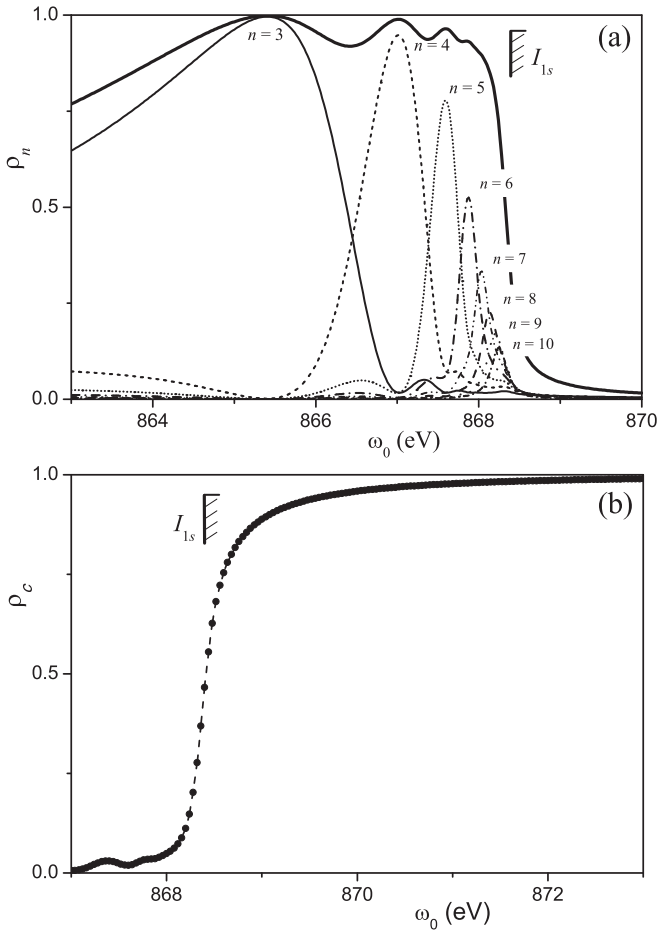

FIG. 1. Hypothesis probability functions for the Ne atom. (a) Top solid curve: sum of functions ρ_n, $\Gamma_{1s} = 0.24$ eV [5]; (b) $\Gamma_{1s} = 0.27$ eV [6]. $I_{1s} = 868.39$ eV (calculation of this work). ω_0 is energy of the photon preparing the $1s2s^22p^6(n,\varepsilon)p$ initial scattering states.

nonphysical loss of photoexcitation intensity (in our case, the loss of creation probability of hypotheses H_n) practically disappears for $n \in [3;50]$.

The analytical structures of $\sigma_n^{(3)}$ and $\sigma_c^{(3)}$ scattering cross sections are expressed via the matrix elements of the $\widehat{Q}$ operator and are defined by the methods in [13]. They will be specified in Sec. III.

Let us conclude Sec. II on the following note. The appearance of a vacancy in the atomic core is accompanied by the radial relaxation effect of ground and excited electronic states [11]. Indeed, the appearance of a deep vacancy leads to the fact that, first of all, the outer shells of the atomic residue react to the destruction of the "screen" between them and the atomic nucleus, significantly reducing their average radius. The displacement towards the nucleus of the atomic residue electron density shells is accompanied by further delocalization of the photoelectron wave function. Estimating the electrostatic interaction time in the hydrogen-like approximation for an average radius $\langle r_{nl}\rangle$ of the valence electron [14] has the form

$$\tau_{ee} = \frac{\langle r_{nl}\rangle}{c}, \quad \langle r_{nl}\rangle = \left(\frac{a_0}{2Z}\right)[3n^2 - l(l+1)], \qquad (17)$$

where the Bohr radius is $a_0 = 5.29 \times 10^{-11}$ m. For the Ne atom ($n = 2, l = 1$) we have $\tau_{ee} \cong 0.10$ as $\ll \tau \ll \tau_{1s}$. Thus, the effect of radial relaxation has enough time to occur given the attosecond contact interaction between the photons and the atom ($\tau \sim 25$ as) studied here. As a result, the probability amplitudes for both radiative and contact transitions are modified. For example, the creation of a $1s$ vacancy in the Ne atom leads to the following transformation of the probability amplitude (12):

$$M_n = N_{1s}\left(\langle 1s_0|\hat{r}|np_+\rangle - \langle 1s_0|\hat{r}|2p_+\rangle\frac{\langle 2p_0|np_+\rangle}{\langle 2p_0|2p_+\rangle}\right), \qquad (18)$$

$$N_{1s} = \langle 1s_0|1s_+\rangle\langle 2s_0|2s_+\rangle^2\langle 2p_0|2p_+\rangle^6. \qquad (19)$$

Here the radial parts of the wave functions of the l_0 states are obtained by solving the nonlinear integral-differential self-consistent-field Hartree-Fock equations for configurations of the atomic ground state; the radial parts of the wave functions of the l_+ states are obtained by solving Hartree-Fock equations for $1s_+2s_+^22p_+^6np_+[^1P_1]$ configurations (in the field of $1s$ vacancy) of the excited atom.

III. RESULTS AND DISCUSSION

The main physical results of this work are presented in Secs. III C and III D. The results of calculations of normal Compton [15] (Sec. III A) and Thomson [16] (Sec. III B) cross sections are presented with the aim of completeness of theoretical description, as well as demonstrating the orders of magnitudes and the forms of triple-differential cross sections for various types of scattering processes. As such, we do not account for the Ne $2p^6$ shell spin-orbit splitting effect because the theoretical value [17] of the constant for such splitting is $\delta_{SO}(2p_{3/2,1/2}) = 0.094\,\text{eV} < \Gamma_{\text{beam}} = 1$ eV (see Fig. 3). Let us next specify the C configurations in Eq. (3) and the analytical structures of the corresponding partial $\sigma_n^{(3)}$- and $\sigma_c^{(3)}$-scattering cross sections in Eq. (5).

A. Normal Compton scattering

Consider the final states of the contact $2s \to xl$ and $2p \to x(l,l+1)$ transitions of the form

$$C \to C_{n_1l_1l} = \begin{cases} 1s\,2s\,2p^6\,np\,xl, & n_1l_1 = 2s, \\ 1s\,2s^2\,2p^5\,np\,x(l,l+1), & n_1l_1 = 2p. \end{cases} \qquad (20)$$

In Eq. (20) and below, x is the energy of the continuum electron. The probability amplitudes of processes (3) for configurations (20) in the Feynman diagram representation of nonrelativistic many-body quantum theory are given in Figs. 2(a) and 2(b).

With our methods from Ref. [13] for the $\sigma_n^{(3)}$-scattering cross section we obtain

$$\sigma_{n,\perp}^{(3)} = r_0^2\,\beta L_n \sum_{n_1l_1\leqslant f}\sum_{l=0}^{\infty}\int_0^{\infty} H_{n_1l_1l}\,G_{n_1l_1l}^{(n)}\,dx, \qquad (21)$$

$$H_{2sl} = (4l+2)R_l^2(2s,xl), \qquad (22)$$

$$H_{2pl} = 6(l+1)\left[R_l^2(2p,x(l+1)) + R_{l+1}^2(2p,xl)\right], \qquad (23)$$

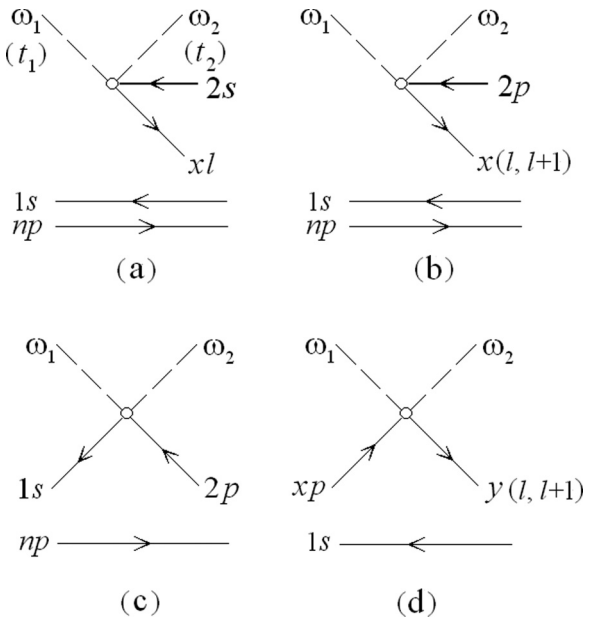

FIG. 2. Probability amplitudes for processes [Eq. (3)] in the Feynman diagram representation: (a) C_{2sl}, (b) C_{2pl}, (c) C_{2pn}, (d) C_{1sy}. Arrow left, vacancy ($\leqslant f$); arrow right, electron ($>f$); open circle is the vertex of the contact interaction over the $\widehat{Q}$ operator. Lower straight lines (unbound parts of the diagrams) are interpreted as the "spectators" of the process. Time direction: left to right ($t_1 < t_2$).

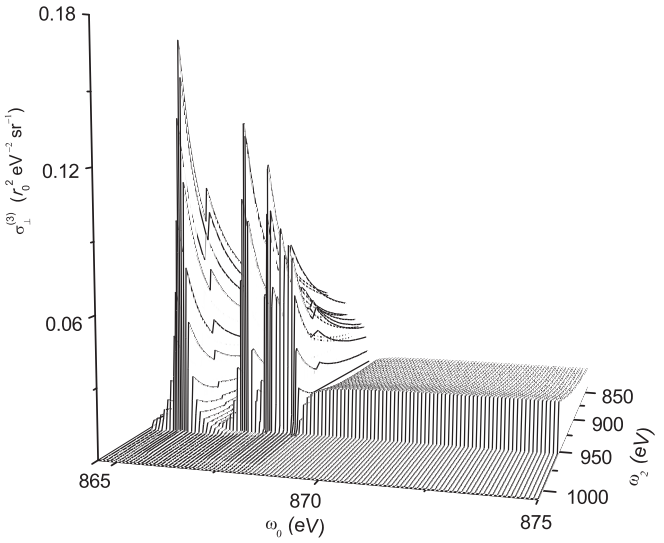

FIG. 3. Triple-differential cross section of the normal Compton scattering of a linearly polarized (perpendicular to the scattering plane, $\perp$) x-ray ω_1 photon by the excited and ionized atom of Ne with attosecond duration of the contact photon-electron interaction. $\omega_1 = 1000$ eV, $I_{1s} = 868.39$ eV, $\Gamma_{1s}(1s \to np) = 0.24$ eV, $\Gamma_{1s}(1s \to \varepsilon p) = 0.27$ eV, $\theta = 90^\circ$, $\Gamma_{\text{beam}} = 1.0$ eV. ω_2 is energy of the scattered photon. Scattering of the ω_1 photon by the εp electron of the continuous spectrum is not taken into account.

$$R_l(a,b) = \langle a|j_l(qr)|b\rangle, \tag{24}$$

$$q = (\omega_1/c)(1+\beta^2-2\beta\cos\theta)^{1/2}, \tag{25}$$

$$G^{(n)}_{n_1l_1l} = \frac{1}{\gamma_b\sqrt{\pi}}\exp\left\{-\left(\frac{\omega_1-\omega_2+I^{(n)}_{n_1l_1}}{\gamma_b}\right)^2\right\}, \tag{26}$$

$$I^{(n)}_{n_1l_1} = E(1s2s^22p^6np) - E\left(C_{n_1l_1l}\right) < 0. \tag{27}$$

In Eqs. (21)–(27), r_0 is the classical electron radius, $\beta = \omega_2/\omega_1$, j_l is the lth-order spherical Bessel function of the first kind, θ is the scattering angle as the angle between wave vectors of the incident ($\vec{k}_1$) and scattered ($\vec{k}_2$) photon, $q = |\vec{k}_1 - \vec{k}_2|$ is the momentum transferred to the excited and ionized atom, G is the Gauss spectral function, $\gamma_b = \Gamma_{\text{beam}}/(2\sqrt{\ln 2})$, Γ_{beam} is the spectral resolution width of the experiment, and E are full Hartree-Fock state energies.

The symbol $\perp$ in Eq. (21) and below corresponds to choosing the following scheme for the proposed experiment of scattering a linearly polarized x-ray photon: $\vec{e}_1||\vec{e}_2$, $\vec{e}_{1,2} \perp P$, where $\vec{e}_1$ ($\vec{e}_2$) is the polarization vector of the incident (scattered) photon, P is the scattering plane, containing vectors $\vec{k}_1$ and $\vec{k}_2$.

For the $\sigma_c^{(3)}$-scattering cross section with the substitute of the np electron of the discrete spectrum by the εp electron of the continuous spectrum in Eq. (20) and in Figs. 2(a) and 2(b) similarly to Eq. (21) we obtain

$$\sigma^{(3)}_{c,\perp} = r_0^2\,\beta S(\omega_0)\sum_{n_1l_1\leqslant f}\sum_{l=0}^{\infty}\int_0^\infty H_{n_1l_1l}\,G_{n_1l_1}\,dx, \tag{28}$$

$$S(\omega_0) = \frac{1}{2\pi\gamma_{1s}}\left[\frac{1}{2}+\frac{1}{\pi}\arctan\left(\frac{\Delta_s}{\gamma_{1s}}\right)+\Delta_s L(0)\right], \tag{29}$$

$$G_{n_1l_1} = \frac{1}{\gamma_b\sqrt{\pi}}\exp\left\{-\left(\frac{\omega_1-\omega_2+\Delta_{n_1l_1}-x}{\gamma_b}\right)^2\right\}, \tag{30}$$

where $S(\omega_0)$ is the spectral function that is transmissive into the region of energies $\omega_0 \geqslant I_{1s}$, $\Delta_s = \omega_0 - I_{1s}$, $\Delta_{n_1l_1} = E(1s2s^22p^6) - [E(1s2s2p^6), n_1l_1 = 2s; E(1s2s^22p^5), n_1l_1 = 2p]$, $\Delta_{n_1l_1} < 0$, $L(0)$, see Eq. (15) with $x = 0$.

Calculation results for the full scattering cross section (5) in the case of normal ($\omega_2 < \omega_1$) Compton scattering with the attosecond duration of the contact photon-electron interaction while accounting for Eqs. (21) and (28) are presented in Fig. 3. The calculated values of I_{1snp} from Eq. (14) are given in Table I.

B. Thomson scattering

In this case, $C = 1s2s^22p^6(n,\varepsilon)p$. Then, for the $\sigma_n^{(3)}$- and $\sigma_c^{(3)}$-scattering cross sections we get, respectively,

(i) $1s \to np$ excitation:

$$\sigma^{(3)}_{n,\perp} = r_0^2\,\beta L_n F_n^2 G_{12}, \tag{31}$$

$$F_n = \sum_{n_1l_1\leqslant np} N_1 R_0(n_1l_1, n_1l_1), \tag{32}$$

TABLE I. Energy thresholds of the $1s \to np$ photoexcitation (I_{1snp}) and intershell $1s2s^22p^6np \to 1s^22s^22p^5np$ transitions [$\Delta_{sp}^{(n)} = E(1s2s^22p^6np) - E(1s^22s^22p^5np)$] for the atom of Ne (calculation of this work).

n	I_{1snp} (eV)	$\Delta_{sp}^{(n)}$ (eV)
3	865.410	848.468
4	867.020	848.519
5	867.602	848.533
6	867.878	848.539
7	868.031	848.541
8	868.124	848.542
9	868.185	848.543
10	868.227	848.544

$$G_{12} = \frac{1}{\gamma_b\sqrt{\pi}} \exp\left\{-\left(\frac{\omega_1 - \omega_2}{\gamma_b}\right)^2\right\}. \quad (33)$$

(ii)$1s \to \varepsilon p$ ionization:

$$\sigma_{c,\perp}^{(3)} = r_0^2\, \beta S(\omega_0) F^2 G_{12}. \quad (34)$$

In Eq. (31) F_n is the form factor (structure function) of the excited atom, N_1 is the filling number of the n_1l_1 shell. In Eq. (34) F is the form factor of the atomic ion with the configuration of $1s2s^22p^6[^2S_{1/2}]$, where the summation over the n_1l_1 shells is bound by the condition $n_1l_1 \leqslant f$. Calculation results for the full scattering cross section (5) for the case of Thomson scattering with attosecond duration of the photon-electron interaction while taking into account Eqs. (31) and (34) are presented in Fig. 4.

C. Anomalous inelastic scattering

In this case let us only consider the configuration $C_{2pn} = 1s^22s^22p^5np$. States [0] (return to the atomic ground state) and $1s^22s2p^6(n,\varepsilon)p$ as the final scattering states were not taken into account, as their sum contribution to the total anomalous inelastic cross section is ~5% of the contribution of $1s^22s^22p^5(n,\varepsilon)p$ configurations. The probability amplitude

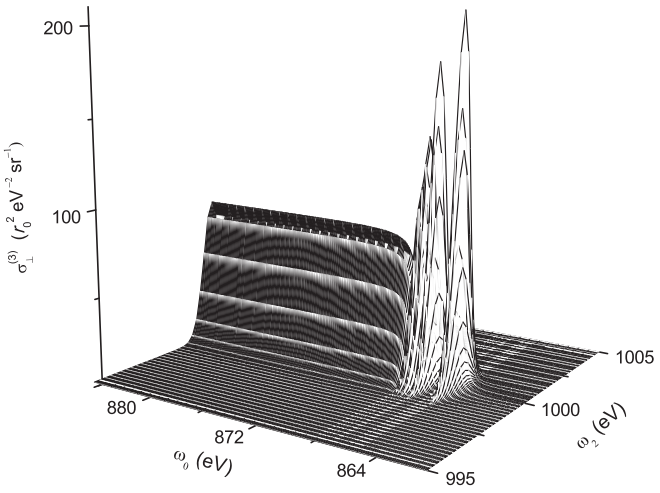

FIG. 4. Same as Fig. 3, but for Thomson scattering.

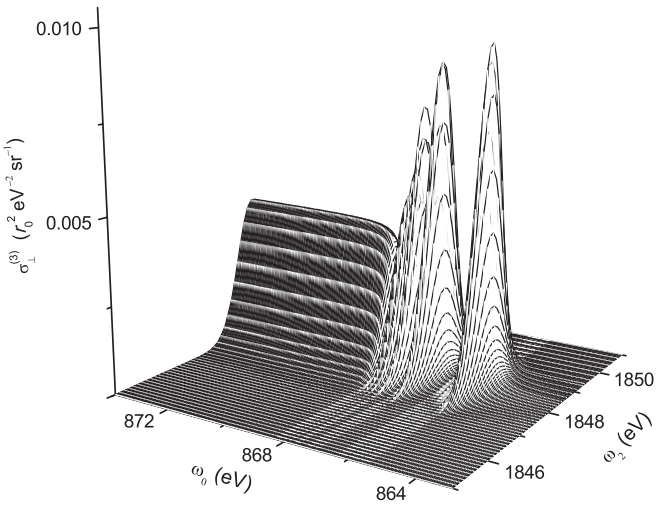

FIG. 5. Same as Fig. 3, but for anomalous inelastic scattering.

of process (3) for configuration C_{2pn} in the Feynman diagram representation is given in Fig. 2(c). For the $\sigma_n^{(3)}$-scattering cross section we obtain

$$\sigma_{n,\perp}^{(3)} = 6r_0^2\, \beta L_n R_1^2(1s,2p) G_{sp}^{(n)}, \quad (35)$$

$$G_{sp}^{(n)} = \frac{1}{\gamma_b\sqrt{\pi}} \exp\left\{-\left(\frac{\omega_1 + \Delta_{sp}^{(n)} - \omega_2}{\gamma_b}\right)^2\right\}, \quad (36)$$

$$\Delta_{sp}^{(n)} = E(1s2s^22p^6np) - E(1s^22s^22p^5np) > 0. \quad (37)$$

For the $\sigma_{c,\perp}^{(3)}$-scattering cross section with the substitution of the discrete spectrum np electron by the continuous spectrum εp electron in the C_{2pn} configuration and in Fig. 2(c) similar to Eq. (35) we obtain

$$\sigma_{c,\perp}^{(3)} = 6r_0^2\, \beta S(\omega_0) R_1^2(1s,2p) G_{sp}, \quad (38)$$

$$G_{sp} = \frac{1}{\gamma_b\sqrt{\pi}} \exp\left\{-\left(\frac{\omega_1 + \Delta_{sp} - \omega_2}{\gamma_b}\right)^2\right\}, \quad (39)$$

$$\Delta_{sp} = E(1s2s^22p^6) - E(1s^22s^22p^5) > 0. \quad (40)$$

Results (35) and (38) generalize those of [3] for the case of constructing a triple-differential scattering cross section and give a description of the quantum effect of anomalous inelastic scattering of the ω_1 photon by an excited and ionized atom: given the attosecond duration of the contact photon-electron interaction, the energy of $1s2s^22p^6(n,\varepsilon)p \to 1s^22s^22p^5(n,\varepsilon)p$ transition is transferred to the ω_1 photon, and does not leave the atomic system via, for example, creation of the ω_3 photon of K_α emission in the radiative decay channel $1s \to 2p^5 + \omega_3$.

The calculation results of the full triple-differential scattering cross section (5) in the case of anomalous inelastic scattering, and taking into account Eqs. (35) and (38), are presented in Fig. 5. The values of Eq. (37) are shown in Table I. Local maxima of the scattering cross section on the energy axis of the ω_2 photon correspond to the zero values of the exponents in Eqs. (36) and (39). Locations of the resonant and

continuous scattering cross-section structures on the energy axis of the ω_0 photon are determined by the values of I_{1snp} and $\omega_0 \geqslant I_{1s}$, respectively. Of course, a decreasing Γ_{beam} in Eqs. (36) and (39) can significantly increase (see, for example, $\sigma_{\perp}^{(3)} \to 10^4\ \sigma_{\perp}^{(3)}$ with $\Gamma_{\text{beam}} = 1$ eV $\to 10^{-4}$ eV [18]) the probability of the experimental observation of the anomalous inelastic scattering effect via intershell transitions in the atomic residue.

D. Scattering from a continuous spectrum electron

Finally, let us consider the process of scattering of the ω_1 photon by an electron of the continuous spectrum of the initial scattering state, not taken into account in Secs. III A, III B, and III C:

$$\omega_1 + 1s2s^2 2p^6 xp \to C_{1sy} + \omega_2, \tag{41}$$

where $C_{1sy} = 1s2s^2 2p^6 y(l,l+1)$. The probability amplitude of process (41) in the Feynman diagram representation is given in Fig. 2(d). In this case, the $1s$ vacancy is left as a "spectator" of the scattering process, and we limit ourselves by taking into account contact transitions into single-electron states of only the continuous ($y \geqslant 0$) spectrum. For the $\sigma_{c,\perp}^{(3)}$-scattering cross section we obtain

$$\sigma_{c,\perp}^{(3)} = r_0^2\,\beta \int_0^{\infty} dy \int_0^{\infty} L(x)\,P(x,y)\,G_{xy}\,dx, \tag{42}$$

$$P(x,y) = \sum_{l=0}^{\infty} (l+1)\left[R_l^2(xp, y(l+1)) + R_{l+1}^2(xp, yl)\right], \tag{43}$$

$$G_{xy} = \frac{1}{\gamma_b \sqrt{\pi}} \exp\left\{-\left(\frac{\omega_1 - \omega_2 + x - y}{\gamma_b}\right)^2\right\}. \tag{44}$$

The convergence of the R_l improper integrals of the first kind of the two radial continuous spectrum wave functions in sum (43) is guaranteed by the oscillating character of the Bessel functions and the fast decay of their magnitudes [19]: $|j_l(z)| \sim z^{-1}$ when $z \to \infty$.

In this work we limit ourselves to the investigation of the limiting form of scattering cross section (42) when $\gamma_{1s} \to 0$, $\gamma_b \to 0$. Then, $L(x) \to \delta(\omega_0 - I_{1s} - x)$ and $G_{xy} \to \delta(\omega_1 - \omega_2 + x - y)$, and instead of Eq. (42) we obtain

$$\overline{\sigma}_{c,\perp}^{(3)} = r_0^2\,\beta\,P(x_0, y_0), \tag{45}$$

$$x_0 = \omega_0 - I_{1s} \geqslant 0, \tag{46}$$

$$y_0 = \omega_1 - \omega_2 + \omega_0 - I_{1s} \geqslant 0. \tag{47}$$

Calculation results for the triple-differential scattering cross section

$$\sigma_{\perp}^{(3)} = \rho_c\,\overline{\sigma}_{c,\perp}^{(3)} \tag{48}$$

are presented in Fig. 6. The energy position of the scattering cross-section structure on the energy axis of the ω_0, ω_2 photons is defined by the hypothesis probability function in Fig. 1(b) and the considerably nonmonotonic behavior of the scattering probability density function $P(x_0, y_0)$. With this, the structure of the scattering cross section (48) presents us with

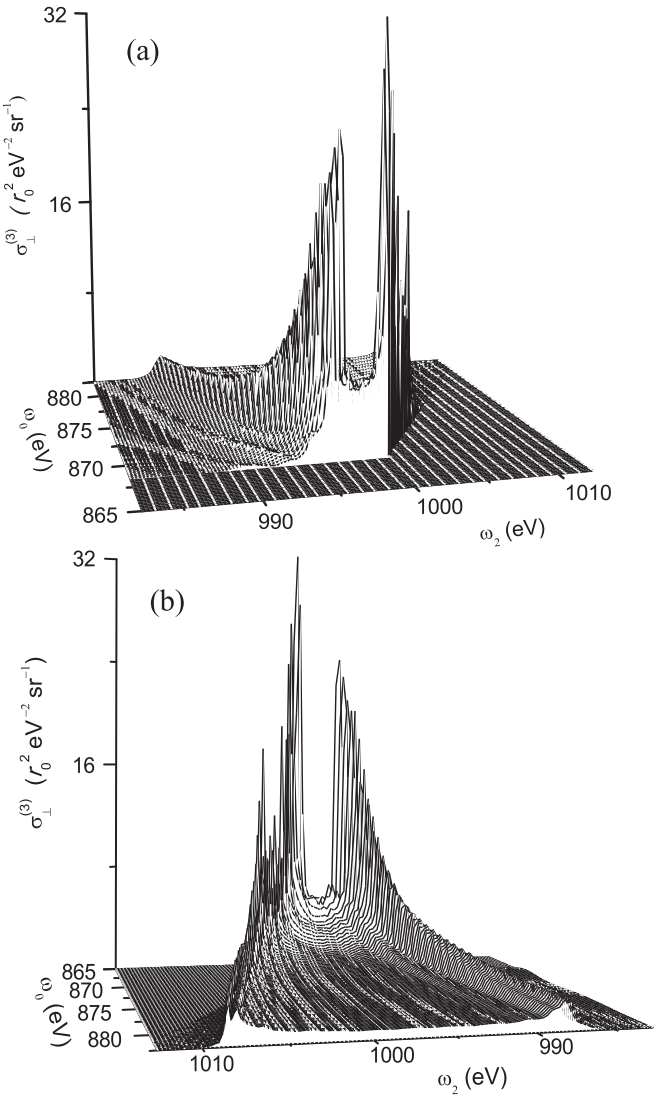

FIG. 6. Triple-differential scattering cross section of a linearly polarized (perpendicular to the scattering plane, $\perp$) x-ray ω_1 photon by the εp electron of the continuous spectrum of the ionized atomic state of Ne in the approximation $\Gamma_{1s} = \Gamma_{\text{beam}} = 0$. (b) Same as (a), but rotated by 180°. The values of ω_1, I_{1s}, and θ are the same as in Fig. 3. ω_2 is the energy of the scattered photon.

a description of two quantum effects of scattering of the ω_1 photon by the ionized atom, which were not investigated in [3].

First effect. In the region of elastic scattering, along with the known contribution of the harmonic $l = 0$ [R_0 with $x_0 = y_0$ in Eq. (43)] of Thomson scattering, appears a contribution of an infinite (and countable) number of harmonics $l \in [1,\infty)$ [R_l with $x_0 = y_0$ in Eq. (43)]. This effect [exclude R_2 for $l = 1$, $x_0 = y_0$ in Eq. (43)] can be interpreted as an effect of changing the l symmetry of the continuous spectrum electron of the final elastic scattering state.

Second effect. Outside of the region of elastic scattering there appears not only the structure of the normal Compton scattering cross section (as a continuation along the energy axis of the ω_2 photon of the scattering cross-section structure in Fig. 3 with $\omega_0 \geqslant I_{1s}$), but also the structure of the anomalous Compton scattering cross section. The existence of the second

effect follows from Eq. (47) as a realization of the double inequality

$$0 \leqslant \omega_2 \leqslant \omega_1 + (\omega_0 - I_{1s}). \tag{49}$$

Indeed, with $\omega_0 > I_{1s}$ an energy region $\omega_2 > \omega_1$ occurs.

Let us give a physical interpretation of Eq. (49) in a different form. Write down the energy conservation law for process (41) in the form:

$$\omega_2 = \omega_1 + (K_1 - K_2), \tag{50}$$

where K_1 (K_2) is the kinetic energy of the continuous spectrum electron of the initial (final) scattering state. Then: (a) when $K_2 > K_1$, the normal Compton scattering regime is defined (final scattering state electron takes away part of the ω_1 photon energy); (b) when $K_2 = K_1$, the regime of elastic (including Thomson) scattering is defined (ω_1 photon is elastically scattered by the initial scattering state electron); (c) when $K_2 < K_1$, the regime of anomalous Compton scattering up to $K_2 = 0$ is defined (all kinetic energy of the initial scattering state electron is transferred to the ω_1 photon: $\omega_2^{\max} = \omega_1 + K_1$, $K_1 = \omega_0 - I_{1s}$). With the increase in the energy of the ω_0 photon (increasing K_1) and a fixed value of energy of the ω_1 photon, the maximum of the normal Compton scattering profile is reduced and shifted into the long-wave energy region of the ω_2 photon relative to the energy value of the elastic scattering [Fig. 6(a)]. An analogous result, but with an evolution into the short-wave energy region of the ω_2 photon, is true for the cross-section profile of the anomalous Compton scattering of the ω_1 photon by the ionized atom [Fig. 6(b)]. With $\gamma_{1s} > 0$ and $\gamma_b > 0$, the said effects are "hidden" in the complex analytical structure of the double improper integral of the first kind [Eq. (42)]. Calculation of this integral is a subject of future investigations.

Let us note that in contrast with the results of Secs. III A, III B, and III C, the existence of both normal Compton and Thomson scattering structures, as well as the described quantum effects in the case of scattering of the ω_1 photon by the continuous spectrum atomic electron, is not limited by the attosecond duration scale of the contact interaction. Indeed, the decay of the $1s$ vacancy as the "spectator" over radiative (e.g., $1s \to 2p^5 + \omega_3$) and Auger autoionization (e.g., $1s \to 2p^4\varepsilon d$) channel types only modifies the Hartree-Fock field for continuous spectrum electrons, but does not take away the fact of their contact interaction with the ω_1 and ω_2 photons. Also note that the effect of anomalous inelastic scattering by an atomic electron of the continuous spectrum is analogous to the same effect but with inverse Compton scattering of the ω_1 photon by a high-energy beam of free electrons (part of the beam energy is transferred to the ω_1 photon and there appears a regime of anomalous Compton scattering). Thus, similar to the results in [2], a theoretical and experimental study of this effect in the case of an ionized atom is of independent interest. In contrast to the results of experiments with a beam of free electrons, dependence of the absolute values and the forms of the scattering cross section (42) on both the nuclear charge and the structure of the infinite set of l symmetries of continuous spectrum atomic electron wave functions should be expected. Indeed, the probability density function $P(x,y)$ in Eq. (43) is defined via the aforementioned infinite set of functions, obtained in a Hartree-Fock field of the fixed atom deep vacancy.

Refinement of the results of Sec. III is concerned, first of all, with solving the problems of analytical construction and taking into account the full orthonormal set of $1s2s^22p^6(n,\varepsilon)p$ states of the atomic excitation and ionization. An example of solving the first problem is given in our recent work [20] (the concept of expanded infinitely dimensional Hilbert space). Solution of the second problem is a subject of future investigations.

Thus, according to the results of Sec. III, two types of processes are found, defining the effect of anomalous inelastic scattering of the ω_1 photon by the excited and ionized atom. *The first type* (Sec. III C): The energy of the intra-atomic transition [Fig. 2(c)] $\Delta_{ps}^{(n)}$ is transferred to the ω_1 photon and there appears a scattered photon of the energy $\omega_2 = \omega_1 + \Delta_{ps}^{(n)} > \omega_1$ (Fig. 5). In this case, already with $\omega_0 \cong I_{1s}$, there happens to be a significant ($\sim$1.85 times for the Ne atom) increase in energy of the ω_1 photon. *The second type* (Sec. III D): The ω_1 photon with $\omega_0 > I_{1s}$ takes away the energy of the continuous spectrum atomic electron [Fig. 2(d)] and there appears a scattered photon of energy $\omega_2 > \omega_1$ (Fig. 6). With $\omega_0 \cong 2I_{1s}$, both processes create a scattered photon of energy $\omega_2 = \omega_1 + \Delta_{ps}^{(n)}$, their probabilities (for $\Gamma_{\text{beam}} \to 0$) nearing each other in the order of magnitude and are summed. There appears a local maximum of probability of the anomalous inelastic scattering effect in the resulting scattering cross section. With $\omega_0 > 2I_{1s}$, as is expected, the main source of the high-energy ($\omega_2 \gg \omega_1$) scattered photons is the second type of process.

Of course, in a possible experiment (e.g., with an x-ray free-electron laser) to discover the effect of anomalous inelastic scattering of the ω_1 photon by an excited and ionized atom, it is necessary to satisfy the condition [3] $t_2 - t_1 \ll \tau_{1s}$. Here, t_1 (t_2) is duration of the ω_0 (ω_1)-photon pulse when realizing two-step scattering processes, investigated in this work. The problem of satisfying this condition is still open.

IV. CONCLUSIONS

Nonrelativistic variant of quantum theory for the process of scattering of an x-ray photon by an excited and ionized atom with attosecond duration of the contact photon-electron interaction is constructed. As the main theoretical result, we predict the quantum effect of anomalous ($\omega_2 > \omega_1$) inelastic scattering. It is also found that the elastic scattering of the photon by an electron of the continuous spectrum is accompanied by the effect of changing the orbital symmetry of the scattered electron. On the example of the Ne atom we obtain the absolute values and the forms of triple-differential cross sections of normal ($\omega_2 < \omega_1$) Compton, elastic ($\omega_2 \cong \omega_1$), and anomalous inelastic scattering in terms of the photon energy that prepares the excitation and ionization states of the atom. The question of an experimental observation of the predicted quantum effects of scattering is left open (see Sec. IV in Ref. [3]).

ACKNOWLEDGMENTS

The authors are grateful to the referees for valuable remarks.

[1] C. Bostedt *et al.*, J. Phys. B **46**, 164003 (2013).
[2] S. Chen *et al.*, Phys. Rev. Lett. **110**, 155003 (2013).
[3] A. N. Hopersky, A. M. Nadolinsky, and S. A. Novikov, Phys. Rev. A **88**, 032704 (2013).
[4] P. A. M. Dirac, *The Principles of Quantum Mechanics* (Clarendon, Oxford, 1958).
[5] A. De Fanis, N. Saito, H. Yoshida, Y. Senba, Y. Tamenori, H. Ohashi, H. Tanaka, and K. Ueda, Phys. Rev. Lett. **89**, 243001 (2002).
[6] M. Coreno, L. Avaldi, R. Camilloni, K. C. Prince, M. de Simone, J. Karvonen, R. Colle, and S. Simonucci, Phys. Rev. A **59**, 2494 (1999).
[7] T. Tanaka, Phys. Rev. Lett. **110**, 084801 (2013).
[8] T. Popmintchev *et al.*, Science **336**, 1287 (2012).
[9] L. D. Landau, Dokl. Akad. Nauk SSSR **60**, 207 (1948) [in Russian]; C. N. Yang, Phys. Rev. **77**, 242 (1950).
[10] W. Feller, *An Introduction to Probability Theory and its Applications* (Wiley, New York, 1970), Vol. 1; D. J. Hudson, *Statistics. Lectures on Elementary Statistics and Probability* (CERN, Geneva, 1964).
[11] M. Ya. Amusia and N. A. Cherepkov, Case Stud. Atom. Phys. **5**, 47 (1975); M. Ya. Amusia, *Atomic Photoeffect* (Plenum, New York, 1990).
[12] A. N. Hopersky, V. A. Yavna, A. M. Nadolinsky, and D. V. Dzuba, J. Phys. B **37**, 2511 (2004).
[13] A. N. Hopersky and A. M. Nadolinsky, Phys. Rev. A **77**, 022712 (2008); J. Exp. Theor. Phys. **115**, 402 (2012).
[14] H. A. Bethe and E. E. Salpeter, *Quantum Mechanics of One- and Two-Electron Atoms* (Dover, New York, 2008).
[15] P. P. Kane, Phys. Rep. **218**, 67 (1992).
[16] P. P. Kane, L. Kissel, R. H. Pratt, and S. C. Roy, Phys. Rep. **140**, 75 (1986).
[17] K.-H. Huang, M. Aoyagi, M. H. Chen, B. Crasemann, and H. Mark, At. Data Nucl. Data Tables **18**, 243 (1976).
[18] Y. Q. Cai *et al.*, J. Phys.: Conf. Ser. **425**, 202001 (2013).
[19] E. Jahnke, F. Emde, and F. Lösch, *Tables of Higher Functions* (McGraw-Hill, New York, 1960).
[20] A. N. Hopersky and A. M. Nadolinsky, J. Phys. B **44**, 075001 (2011).